Effects of metal oxide surface doping with phosphonic acid monolayers on alcohol dehydration activity and selectivity

Lucas D. Ellis[1], Jordi Ballesteros-Soberanas[1], Daniel K. Schwartz[1], J. Will Medlin[1*]

[1]Department of Chemical & Biological Engineering,

University of Colorado Boulder, Boulder, CO 80309-0596

*Corresponding author, email: Will.Medlin@colorado.edu

Keywords: metal oxide catalysis, alcohol dehydration, self-assembled monolayers, phosphonic acids.

Abbreviations: SAMs = self-assembled monolayers, MPA = methylphophonic acid, ODPA = octadecylphosphonic acid.

Abstract

Controlling the near-surface environment of heterogeneous catalysts is of fundamental importance for high selectivity and activity. Self-assembled monolayers (SAMs) are effective tools to control reaction selectivity and activity for both supported noble metal and metal oxide catalysts. We previously demonstrated tunable dehydration activity of alcohols on phosphonic acid-modified, anatase-phase TiO_2. In this work, we investigated the generality of this approach by studying the modification of other metal oxides including Al_2O_3, CeO_2, CuO, Fe_2O_3, MgO, rutile-TiO_2, SnO_2, V_2O_5, WO_3, ZrO_2, and ZnO. Modification of these materials with phosphonic acids results in the formation of SAMs on the surface, as determined by infrared spectroscopy; studies of the thermal stability on selected catalysts indicated that the SAMs remained intact up to approximately 400°C in inert environments. Decomposition of alcohols on these native materials resulted in dehydration, dehydrogenation, and condensation. Upon functionalization with phosphonic acid modifiers, the activity of all pathways decreased significantly, except for dehydration on CeO_2, anatase-TiO_2, and SnO_2. We explored the properties of these oxides that may be responsible for this increase in dehydration activity using correlations to bulk properties. This analysis supported the hypothesis that phosphonic acid monolayers act as surface-level dopants for metal oxides of specific metal-oxygen bond strength and oxidation state.

1. Introduction

Understanding and controlling the near-surface environment is of critical importance in the field of catalysis. One recently developed strategy involves the use of self-assembled monolayers (SAMs) to tune the surface chemistry of catalysts.[1,2] Self-assembled monolayers and similar modifiers have gained recent interest because of their enhancement of catalytic selectivity and activity.[3–7] Recent studies have sought to extend these SAM strategies to metal oxide catalysts and supports using silane[8] and phosphonate modifiers.[9,10] However, these efforts focused only on Al_2O_3 and TiO_2. Phosphonic acids have been shown to form SAMs on a wide variety of metal oxides, providing potential opportunities to expand this SAM strategy to a broad set of reaction chemistries.

In this work, we explored the effect of phosphonate SAMs on the reactivity of alcohols on a wide variety of metal oxide catalysts functionalized with alkyl phosphonic acids. We found that phosphonates were able to form organized and robust SAMs on many metal oxides. Activity toward decomposition of linear alcohols was promoted on anatase phase TiO_2, SnO_2 and CeO_2, but not other oxides. In fact, most oxides demonstrated a significant reduction in catalytic activity for all reaction pathways. Through correlations with bulk properties, we propose that phosphonates acted as surface level dopants, tuning the activity of alcohol dehydration, for a specific set of oxides.

2. Experimental

2.1 Catalyst synthesis

All metal oxide powders were purchased commercially: iron (III) oxide, NanoArc, (CAS: 1309-37-1, LOT: L20Y042, Alfa Aesar), Copper (II) oxide, min. 97%, 99+% Cu (CAS:1317-38-0, LOT: 28673900, Strem Chemicals Inc.), zinc (II) oxide, 99.7% (CAS: 1314-13-2, LOT: A9680109, Strem Chemicals Inc.), titanium (IV) oxide, rutile, 99.8% (CAS:1317-80-2, LOT: T24A025, Alfa Aesar), tungsten (VI) oxide, 99.9% (CAS: 1314-35-8, LOT: BCBN7138V, Fluka Analytical, Sigma Aldrich), titanium (IV) oxide, ≥99% trace (CAS: 1317-70-0, LOT: MKCF0054, Aldrich Chemistry, Sigma Aldrich), cerium (IV) oxide, 99.5% min (CAS: 1306-38-3, LOT: D06X036, Alfa Aesar), magnesium (II) oxide, 99+% (metals basis) (CAS:1309-48-4, LOT: M20B021, Alfa Aesar), tin (IV) oxide, 99.9% (metals basis) (CAS: 18282-10-5, LOT: R20B037, Alfa Aesar), and zirconium (IV) oxide, 99% trace metals (CAS: 1314-23-4, LOT: BCBM6158V, Aldrich Chemistry, Sigma Aldrich).

Metal oxide powders were functionalized with methylphosphonic acid, 98% (CAS: 993-13-5, LOT: 10206487, Alfa Aesar) and octadecylphosphonic acid, by mixing metal oxides in a 10mM solution in tetrahydrofuran (THF), HPLC Grade (CAS: 109-99-9, LOT: 177753, Fisher Chemicals) overnight. Powders were removed from solution via centrifugation, decanting excess solvent and annealing at 120°C for 6 hours. Powders were then rinsed with the same volume as the deposition volume of THF three times before drying the samples overnight under vacuum.

2.2 Catalyst Characterization

Atmospheric diffuse reflectance infrared Fourier transform spectroscopy (DRIFTS) was performed on a Praying Mantis system (Harrick Scientific). Reported DRIFTS results represent the raw spectra, and are not normalized between samples. Surface area measurements were performed using nitrogen physisorption (30% nitrogen, balance helium, Airgas), unless surface areas were reported by the manufacturer. Inductively coupled plasma mass spectrometry (ICP-MS) was performed to measure phosphorous and cation content of native and functionalized materials. Temperature programmed reaction spectroscopy (TPRS) and temperature programmed desorption (TPD) were performed using a custom quartz tube (6.35-mm inner diameter) vapor phase reactor. The effluent was monitored with a Pfeiffer mass spectrometer. For TPD experiments, functionalized catalysts were sandwiched between two 125mg slugs of quartz wool with either ultra-high purity (UHP) helium (Airgas), or 7 torr water vapor in UHP helium as a carrier gas. Temperature programmed desorption started at 100°C and ended at 550°C with a ramp rate of 10°C/min. For TPRS experiments, catalysts were sandwiched between 125mg of quartz wool and pretreated in UHP helium for 1 hr at 250°C. After pretreatment, samples were cooled to 50°C, then saturated with 1-butanol vapor in UHP helium for 10 minutes. The system was then purged for 25 minutes before beginning the 20°C/min ramp rate to 550°C.

2.3 Catalyst Performance

Reactions of 1-butanol were conducted on a custom pyrex-tube (6.35-mm inner diameter) packed bed vapor phase reactor with an Agilent gas chromatograph with a thermal conductivity and flame-ionization detector measuring effluent concentrations of reactants and products. A DB-WAX (30m x 0.250mm x 0.50μm) column was used to separate components. The reactant, 1-butanol (≥ 99%, for molecular biology, Sigma-Aldrich), was delivered to the catalyst by bubbling an inert carrier (helium, ultra high purity, Airgas) through the liquid phase reactant, which was temperature controlled with a water bath set to 14°C. Reactions were performed at 250°C with data reported for data acquired from 180-210 minutes (time-on-stream) then averaged with two other sample replicates. Experimental uncertainty is represented as the standard error from triplicate samples.

3. Results

3.1 Catalyst Characterization

Metal oxide powders (Table 1) were functionalized with octadecylphosphonic acid (ODPA) and methylphosphonic acid (MPA). Here, we used ODPA modification as a method to test whether relatively close-packed monolayers were formed on the various surfaces. Functionalization of materials with long-chain alkyl SAMs like ODPA can be thoroughly studied and the organization of these SAMs is often characterized using asymmetric and symmetric vibrational modes of methylene functionalities.[10] The frequencies

for these vibrations redshift as the SAM molecules become more organized. Figure 1 shows the infrared spectra of the ODPA-functionalized metal oxides. All modified oxides studied here demonstrated an asymmetric methylene vibrational frequency typical of organized SAMs. Organization does appear to depend to some extent on the metal oxide; while many metal oxides have clear peaks at 2920 cm^{-1} or lower, V_2O_5, ZrO_2, TiO_2 rutile showed more blue-shifted peaks associated with decreased organization. To our knowledge, this is the first report of the functionalization of CeO_2, CuO, MgO, SnO_2, and V_2O_5 with phosphonic acids. Functionalization of Al_2O_3,[11–13] Fe_2O_3,[14] TiO_2,[11–13,15] WO_3,[16] ZrO_2,[11,12,17] and ZnO [18–21] has been reported previously, however.

An important criterion for the use of SAM-modified catalysts is that the coating must remain stable at reaction temperatures of interest. Few studies have focused on the thermal stability of phosphonic acid functionalized metal oxides with a couple exceptions.[13,22] McElwee et al. utilized thermogravimetric analysis to demonstrate no degradation of ODPA-functionalized γ-Al_2O_3 and TiO_2-anatase powders below 430°C. Bhairamadgi et al. noted no degradation of ODPA-functionalized porous alumina below 500°C. We expanded the range of oxides investigated and explored the stability of ODPA functionalized γ-Al_2O_3, TiO_2-anatase, ZrO_2, and ZnO using DRIFTS of the C-H stretching region (supplementary information, Figure S1) and temperature programmed desorption (TPD) (supplementary information, Figure S2). Temperature programmed desorption in helium and 1% water vapor in helium demonstrated no production of volatile decomposition products below 400°C.

We also investigated the organization of the ODPA tail functionality using temperature- and atmosphere-controlled DRIFTS. In a helium atmosphere, little degradation of asymmetric or symmetric methylene vibrations was measured after heating the sample to ~400°C and returning to ambient conditions. These results were in line with previous studies of reactions of alcohols on phosphonic acid functionalized TiO_2- and Al_2O_3-based catalysts, which showed no loss of functionality after exposure to reaction conditions.[9,23,24] We noted that there were subtle shifts in peak frequency and intensity after the thermal treatment; as shown in Figure S1, for example, the peak intensity for methylene stretching in some cases increased after heating. Such changes have previously been interpreted in terms of reorganization of the monolayers to adopt different orientations (e.g., with different degrees of tilt) during annealing.[25] Though these SAMs were found to be stable to 400°C in inert environments and in the presence of low levels of water vapor, it should be noted that harsher (especially oxidizing) conditions may lead to degradation.

Although the DRIFTS results are generally consistent with a relatively full monolayer, some coverage variations between the different oxides are expected. Inductively coupled plasma (ICP) techniques have been used to estimate the coverage of several phosphonic acids on Al_2O_3 to be approximately 3-4 molecules nm^{-2}, and analysis of benzyl phosphonic acids on TiO_2 have indicated a similar coverage.[9,13,24] Attempts to accurately measure coverage changes across different oxides with ICP in this study were hampered by the low surface areas of many of the tested materials. In addition to the possibility of changes in

surface coverage, it is important to note that different oxides have been reported to yield different modes of phosphonate attachment.[17]

3.2 Catalyst Performance

Previously, we demonstrated that there was a weak inverse dependence of alkyl tail length and dehydration activity, where shorter moieties, like MPA functionalized anatase phase TiO_2 had higher dehydration activity compared with decylphosphonic- and ODPA-functionalized TiO_2.[9] With these findings in mind, we sought to determine which oxides demonstrated maximal dehydration activity, by focusing on MPA functionalized materials.

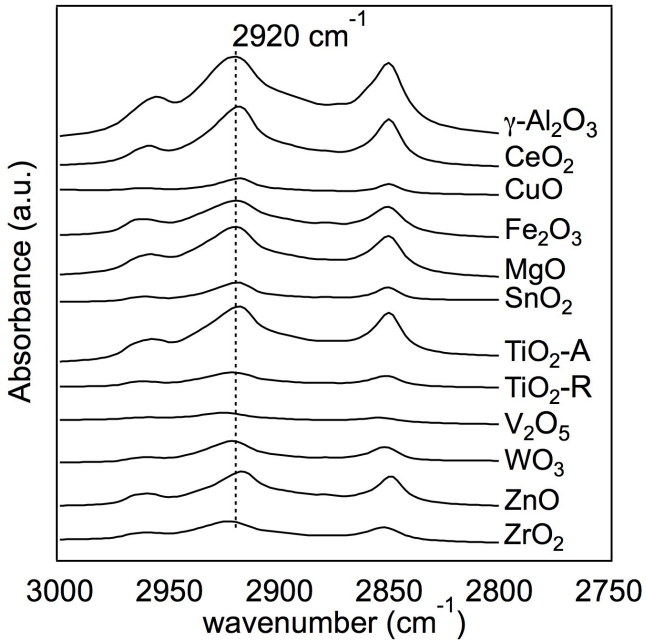

Figure 1 DRIFTS spectrum of ODPA functionalized oxides in the C-H stretching region.

Table 1 Summary of crystal structure and BET surface area of metal oxides used in this study.

Catalysts	Crystal Type	BET Surface Area

		m2/g
γ-Al_2O_3	hexagonal	56
CeO_2	cubic	60
CuO	monoclinic	3.2
Fe_2O_3	cubic	30
MgO	cubic	1.5
SnO_2	tetragonal	5.1
TiO_2-anatase	tetragonal	9.0
TiO_2-rutile	tetragonal	4.9
V_2O_5	orthorhombic	3.4
WO_3	monoclinic	3.0
ZnO	hexagonal Wurtzite	1.3
ZrO_2	monoclinic	3.1

Metal oxide powders functionalized with MPA were compared to their native counterparts in the vapor-phase decomposition of 1-butanol at 250°C using a helium gas carrier. Primary alcohols are known to react via dehydration, dehydrogenation, and condensation on metal oxides. Condensation is often a minor pathway, with selectivities typically below 15%. However, γ-Al_2O_3 is a notable exception to this trend, since the ether made up nearly 60% of the products at these reaction conditions, as expected.[26] After functionalization with MPA, significant selectivity changes (>15%) occurred for five materials: γ-Al_2O_3, TiO_2-anatase, CeO_2, V_2O_5, and SnO_2 (Figure 2). The greatest changes (>30%) occurred for γ-Al_2O_3, TiO_2-anatase, and SnO_2. Anatase-phase TiO_2 and SnO_2 demonstrated increases in dehydration selectivity (>50%) and decreases in dehydrogenation selectivity (>50%), while γ-Al_2O_3 exhibited decreases in condensation (>30%) and increases in dehydration (>30%). Ceria and V_2O_5 also saw a respective 13.6% and 20.5% decrease in dehydrogenation selectivity and 15.6% and 17.1% increase in dehydration selectivity, with a difference between these pathways coming from a change in condensation selectivity (Figure 2 and

supplementary information Figure S3). All other oxides showed little to no change in reaction selectivity beyond experimental error.

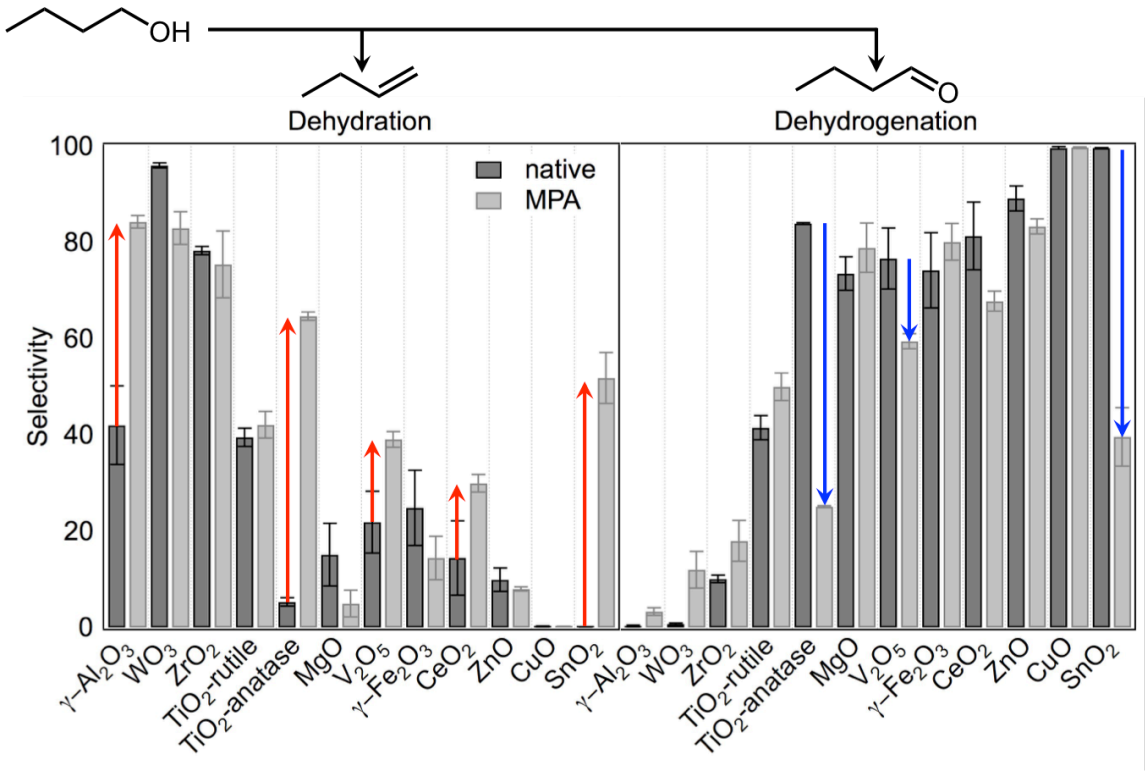

Figure 2 Selectivity to dehydration and dehydrogenation products for 1-butanol reaction at 250°C. Red arrows indicated increases in selectivity of >30%, while blue arrows indicate decreases in selectivity of >30% after functionalization with MPA.

The selectivity trends show that γ-Al_2O_3, TiO_2-anatase, V_2O_5, SnO_2 and CeO_2 were outliers in performance after functionalization with MPA. However, upon closer examination of reaction rates, a new and more surprising trend emerged (Figure 3). Gamma-alumina demonstrated a decrease in activity for dehydration, dehydrogenation, and condensation. In fact, activities for all pathways decreased by nearly 99%, indicating that the phosphonates were highly effective surface poisons. Activity for each pathway also decreased for coated V_2O_5, but to a lesser extent. For CeO_2, SnO_2, and TiO_2-anatase, dehydration activity increased, while dehydrogenation and condensation activity

decreased. In fact, dehydration activity increased by 110%, 210% and 810% while dehydrogenation activity decreased by 26%, 92% and 99% for CeO_2, TiO_2-anatase, and SnO_2, respectively. Because of the high selectivity to the dehydrogenation product for uncoated CeO_2 and SnO_2, the significant increase in dehydration rates was not accompanied by high selectivities. For example, native SnO_2 had a 99.7% selectivity toward the dehydrogenation product; modification with MPA therefore only improved the dehydration selectivity to approximately 50%. Overall, these results raised two questions: (1) Why is the dehydration pathway promoted while dehydrogenation and condensation decrease in activity? and (2) What oxide properties are associated with an increase in dehydration activity after MPA functionalization?

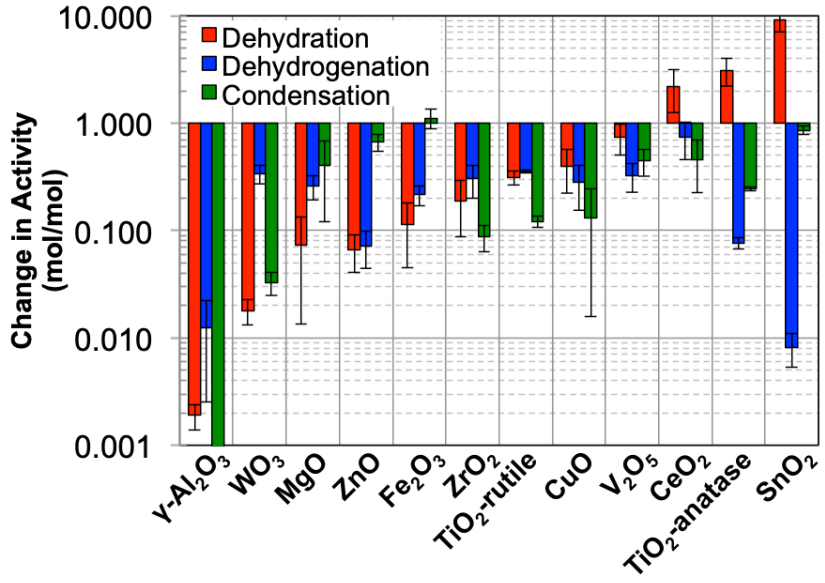

Figure 3. Ratio in activity of dehydration, dehydrogenation, and condensation comparing phosphonate functionalized metal oxide divided by the native performance in the reaction of 1-butanol at 250°C.

3.3 Influence of phosphonates on surface chemistry

Previous studies of reactions of 1-propanol on anatase TiO_2 demonstrated a 13 kJ/mol decrease in the apparent activation energy for dehydration and a 42 kJ/mol increase for dehydrogenation for the MPA functionalized material.[9] This suggested a significant shift in the energetic landscape of the dehydrogenation mechanism with a moderate shift in the dehydration mechanism. Dehydrogenation is thought to require two Lewis acid sites, the first capable of binding the alcohol and the second abstracting a hydride alpha to the alcohol carbon.[27–29] The functionalization with phosphonic acids would be expected to reduce the number of two adjacent Lewis acids, thus lowering selectivity to dehydrogenation. The argument is similar for condensation, a bimolecular reaction. For condensation to occur two alcohols must adsorb near to one another; having a high concentration of phosphonic acids on the surface likely reduces the probability for such an occurrence.

The phosphonic acid surface coverage is consistent with the decrease in dehydrogenation and condensation activity, but does not explain the varying response in dehydration activity. More explicitly, dehydration activity appears to have no correlation with surface coverage. Using temperature programmed reaction spectroscopy (TPRS) (supplementary information Figures S4-S5) we noted a significant reduction in the total adsorption of alcohols on all materials, again, consistent with high surface coverage of phosphonic acids. Moreover, the available alcohol binding sites appear to have comparable adsorption strength to the native counterpart. It therefore appears the phosphonic acids must increase

intrinsic activity of the remaining sites for dehydration, but only for specific oxides. We sought to explain this result by correlations to bulk material properties.

4. Discussion

It is useful to consider results from previous studies that have sought to identify the relationship between metal oxide properties and reaction performance. Previous studies have provided an in-depth analysis of metal oxide properties as they impact dehydrogenation activity of simple alcohols like ethanol.[30,31] Idriss el al. investigated correlations of dehydrogenation activity with bulk metal oxide properties such as electronegativity difference between the metal and oxygen, metal oxygen bond strength, oxygen partial charge, oxygen Madelung potential, and oxygen electronic polarizability, and concluded that the oxygen electronic polarizability was the best predictor for dehydrogenation activity. We sought to utilize similar material properties: differences in electronegativity between the metal and oxide, polarizability of the cation, polarizability of the oxide, band gap, and metal oxygen bond strength, as possible descriptors for the change in dehydration activity of these materials after functionalization with phosphonic acid modifiers. Differences in metal oxide electronegativities and polarizability of the cation and oxide did not demonstrate a significant correlation (supplementary information, Figures S6-S9). Use of the metal-oxygen bond strength as a descriptor resulted in a “volcano” type relationship, with strong and weak metal oxygen bond strengths having the most suppression in dehydration activity after functionalization with phosphonic acids,

while moderate metal-oxygen bond strength materials had improved activity levels. The use of metal-oxygen bond strength as a predictor does have a connection to the mechanism of dehydration, since metal-oxygen bond cleavage is thought to occur during the E2-like surface mediated reaction.[32,33] As discussed in more detail below, there are a few key outliers in this relationship, suggesting that other factors likely play a role in dictating how phosphonate dopants influence catalysis.

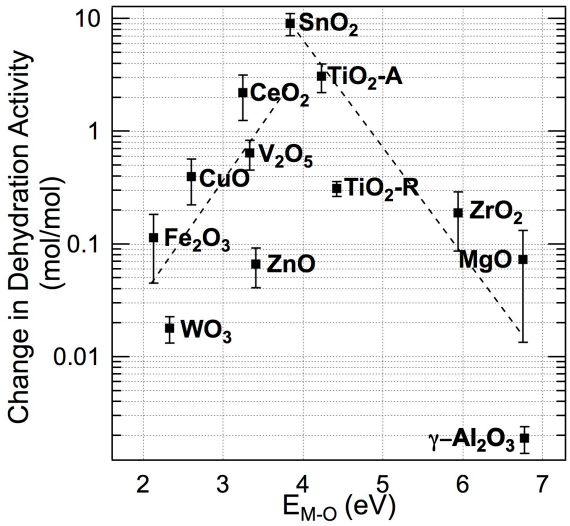

Figure 4 Change in dehydration activity after functionalization with MPA as a function of the difference of metal oxygen bond strength (E_{M-O}) taken from Helali et al. and Idriss et al.. [31,34]

The complex response of dehydration activity and functionalization with phosphonic acids appears to be correlated with electron mobility and energetics. Though phosphonic acids have not be used for this express purpose (i.e., tuning catalytic properties of surface atoms), phosphonic acids have been understood to tune the work function of electronic materials like zinc oxide[19,20] and indium tin oxide.[35–38] Metiu et al.[39] demonstrated that surface-level cation exchange in metal oxides can provide a means to control Lewis acid and base properties. For example, by replacing a surface level cation with one of higher valance, the

surface can become more of a Lewis base, hypothetically enhancing activity toward elimination of the beta hydrogen of the alcohol.[32] This newly doped surface will result in stronger binding of Lewis acids, but weaker binding of Lewis bases. Interestingly, this type of analysis on our materials highlights one critical common factor among the three oxides, CeO_2, SnO_2, and TiO_2: all oxides have the same bulk metal oxidation state. Binding of the phosphonic acids on the surface of these oxides could be seen as a type of surface doping with phosphorous being the cation of higher oxidation state. With this hypothesis in mind, according the rules developed by Metiu et al., phosphorous would act as a high valence dopant, resulting in a surface with weaker binding to Lewis bases. Since alcohols are Lewis bases, this hypothesis suggests a significant weakening in the adsorption energy of alcohols. Unfortunately, attempts to investigate surface acidity using ammonia TPD were complicated by very low yields observed (supplementary information Table S1); we also were unable to resolve trends in surface hydroxyl stretching modes on the various oxides (supplementary information Figure S10).

One obvious outliner in our trends is the comparison of anatase and rutile phase TiO_2. Rutile demonstrated a decrease in dehydration activity of 69% while anatase phase TiO_2 demonstrated an increase of over 200%. Though these two materials appear to share many similar qualities, there is precedent for significant variation in catalytic activity of these materials related to electronic structure differences, as well as major differences in the interaction of surface dopants.[40,41]

5. Conclusions

Phosphonic acid monolayers are capable of forming robust monolayers on many different metal oxide powders. However, the change in catalytic activity, specifically for alcohol dehydration, was limited to TiO_2-anatase, CeO_2 and SnO_2. We speculate the reason is due to electronic doping by the phosphonic acid monolayers. The bulk properties that seem important to this process relate to metal-oxygen bond strength of a certain range and oxidation state. Clearly more studies are required to fully elucidate the mechanistic understanding of this phenomena, but this study does highlight the use phosphonic acid monolayers as robust dopants for certain thermochemical conversions of oxygenates by metal oxide catalysts.

6. Acknowledgements

The authors would like to acknowledge financial support from the United States Department of Agriculture, National Institute of Food and Agriculture predoctoral fellowship program (Award Number #: 2017-67011-26078) and the Department of Energy, Office of Science, Basic Energy Sciences Program, Chemical Sciences, Geosciences and the Biosciences Division (Grant No. DE-FG02-10-ER16206).

7. References

[1] S.T. Marshall, M. O'Brien, B. Oetter, A. Corpuz, R.M. Richards, D.K. Schwartz, J.W. Medlin, Nat. Mater. 9 (2010) 853–858.

[2] C. a Schoenbaum, D.K. Schwartz, J.W. Medlin, Acc. Chem. Res. 47 (2014) 1438–45.

[3] B. Wu, H. Huang, J. Yang, N. Zheng, G. Fu, Angew. Chem. Int. Ed. Engl. 51 (2012) 3440–3443.

[4] S.G. Kwon, G. Krylova, A. Sumer, M.M. Schwartz, E.E. Bunel, C.L. Marshall, S. Chattopadhyay, B. Lee, J. Jellinek, E. V. Shevchenko, Nano Lett. 12 (2012) 5382–5388.

[5] C.-H. Lien, J.W. Medlin, J. Phys. Chem. C 118 (n.d.) 23783–23789.

[6] I. Schrader, J. Warneke, J. Backenköhler, S. Kunz, J. Am. Chem. Soc. 137 (2015) 905–912.

[7] G. Chen, C. Xu, X. Huang, J. Ye, L. Gu, G. Li, Z. Tang, B. Wu, H. Yang, Z. Zhao, Z. Zhou, G. Fu, N. Zheng, Nat. Mater. 15 (2016) 564.

[8] L.D. Ellis, S. Pylypenko, S.R. Ayotte, D.K. Schwartz, J.W. Medlin, Catal. Sci. Technol. 6 (2016) 5721–5728.

[9] L.D. Ellis, R.M. Trottier, C.B. Musgrave, D.K. Schwartz, J.W. Medlin, ACS Catal. 7 (2017) 8351–8357.

[10] T. Van Cleve, D. Underhill, M. Veiga Rodrigues, C. Sievers, J.W. Medlin, Langmuir 34 (2018) 3619–3625.

[11] W. Gao, L. Dickinson, C. Grozinger, F.G. Morin, L. Reven, Langmuir 12 (1996) 6429–6435.

[12] R. Hofer, M. Textor, N.D. Spencer, Langmuir 17 (2001) 4014–4020.

[13] J. McElwee, R. Helmy, A.Y. Fadeev, J. Colloid Interface Sci. 285 (2005) 551–556.

[14] C. Yee, G. Kataby, A. Ulman, T. Prozorov, H. White, A. King, M. Rafailovich, J. Sokolov, A. Gedanken, Langmuir 15 (1999) 7111–7115.

[15] G. Guerrero, P.H. Mutin, A. Vioux, Chem. Mater. 13 (2001) 4367–4373.

[16] F.H. Li, J.D. Fabbri, R.I. Yurchenko, A.N. Mileshkin, J.N. Hohman, H. Yan, H. Yuan, I.C. Tran, T.M. Willey, M. Bagge-Hansen, J.E.P. Dahl, R.M.K. Carlson, A.A. Fokin, P.R. Schreiner, Z.-X. Shen, N.A. Melosh, Langmuir 29 (2013) 9790–9797.

[17] W. Gao, L. Dickinson, C. Grozinger, F.G. Morin, L. Reven, Langmuir 13 (1997) 115–118.

[18] B. Zhang, T. Kong, W. Xu, R. Su, Y. Gao, G. Cheng, Langmuir 26 (2010) 4514–4522.

[19] P.J. Hotchkiss, M. Malicki, A.J. Giordano, N.R. Armstrong, S.R. Marder, J. Mater. Chem. 21 (2011) 3107.

[20] I. Lange, S. Reiter, M. Pätzel, A. Zykov, A. Nefedov, J. Hildebrandt, S. Hecht, S. Kowarik, C. Wöll, G. Heimel, D. Neher, Adv. Funct. Mater. 24 (2014) 7014–7024.

[21] R. Quiñones, D. Shoup, G. Behnke, C. Peck, S. Agarwal, R.K. Gupta, J.W. Fagan, K.T. Mueller, R.J. Iuliucci, Q. Wang, Materials (Basel). 10 (2017).

[22] N.S. Bhairamadgi, S.P. Pujari, F.G. Trovela, A. Debrassi, A.A. Khamis, J.M. Alonso, A.A. Al Zahrani, T. Wennekes, H.A. Al-Turaif, C. van Rijn, Y.A. Alhamed, H. Zuilhof, Langmuir 30 (2014) 5829–5839.
[23] J. Zhang, L.D. Ellis, B. Wang, M.J. Dzara, C. Sievers, S. Pylypenko, E. Nikolla, J.W. Medlin, Nat. Catal. (2018) 1.
[24] P.D. Coan, L.D. Ellis, M.B. Griffin, D.K. Schwartz, J.W. Medlin, J. Phys. Chem. C 122 (2018) 6637–6647.
[25] A.R. Corpuz, S.H. Pang, C. Schoenbaum, J.W. Medlin, Langmuir 30 (2014) 14104–14110.
[26] H. Knözinger, A. Scheglila, J. Catal. 17 (1970) 252–263.
[27] J.E. Rekoske, M.A. Barteau, J. Catal. 165 (1997) 57–72.
[28] H. Idriss, in: R. Rioux (Ed.), Model Syst. Catal., Springer New York, 2010, pp. 133–154.
[29] A.M. Nadeem, G.I.N. Waterhouse, H. Idriss, Catal. Today 182 (2012) 16–24.
[30] H. Idriss, M.A. Barteau, Adv. Catal. 45 (2000) 261–331.
[31] H. Idriss, E.G. Seebauer, Catal. Letters 66 (2000) 139–145.
[32] P. Kostestkyy, J. Yu, R.J. Gorte, G. Mpourmpakis, Catal. Sci. Technol. 4 (2014) 3861–3869.
[33] P. Kostetskyy, G. Mpourmpakis, Catal. Sci. Technol. 5 (2015) 4547–4555.
[34] Z. Helali, A. Jedidi, O.A. Syzgantseva, M. Calatayud, C. Minot, Theor. Chem. Acc. 136 (2017).
[35] M. Gliboff, H. Li, K.M. Knesting, A.J. Giordano, D. Nordlund, G.T. Seidler, J.-L. Brédas, S.R. Marder, D.S. Ginger, J. Phys. Chem. C 117 (2013) 15139–15147.
[36] S.E. Koh, K.D. McDonald, D.H. Holt, C.S. Dulcey, J.A. Chaney, P.E. Pehrsson, Langmuir 22 (2006) 6249–6255.
[37] H. Li, P. Paramonov, J.-L. Bredas, J. Mater. Chem. 20 (2010) 2630.
[38] S.A. Paniagua, P.J. Hotchkiss, S.C. Jones, S.R. Marder, A. Mudalige, F.S. Marrikar, J.E. Pemberton, N.R. Armstrong, J. Phys. Chem. C 112 (2008) 7809–7817.
[39] H. Metiu, S. Chrétien, Z. Hu, B. Li, X. Sun, J. Phys. Chem. C 116 (2012) 10439–10450.
[40] M. Batzill, Energy Environ. Sci. 4 (2011) 3275.
[41] C. Hernandez-Mejia, E.S. Gnanakumar, A. Olivos-Suarez, J. Gascon, H.F. Greer, W. Zhou, G. Rothenberg, N.R. Shiju, Catal. Sci. Technol. 6 (2016) 577–582.